

HEB heterodyne focal plane arrays: a terahertz technology for high sensitivity near-range security imaging systems*

Eyal Gerecht^{**a}, Dazhen Gu^a, Sigfrid Yngvesson^b, Fernando Rodriguez-Morales^b, Ric Zannoni^b, and John Nicholson^b

^aNational Institute of Standards and Technology, Boulder, CO 80305;

^bDepartment of Electrical and Computer Engineering, University of Massachusetts at Amherst, MA 01003

ABSTRACT

We have achieved the first demonstration of a low-noise heterodyne array operating at a frequency above 1 THz (1.6 THz). The prototype array has three elements, consisting of NbN hot electron bolometer (HEB) detectors on silicon substrates. We use a quasi-optical design to couple the signal and local oscillator (LO) power to the detector. We also demonstrate, for the first time, how the HEB detectors can be intimately integrated in the same block with monolithic microwave integrated circuit (MMIC) IF amplifiers. Such focal plane arrays can be increased in size to a few hundred elements using the next generation fabrication architecture for compact and easy assembly. Future HEB-based focal plane arrays will make low-noise heterodyne imaging systems with high angular resolution possible from 500 GHz to several terahertz. Large low-noise HEB arrays are well suited for real-time video imaging at any frequency over the entire terahertz spectrum. This is made possible by virtue of the extremely low local oscillator power requirements of the HEB detectors (a few hundred nanowatts to a microwatt per pixel). The operating temperature is 4 to 6 K, which can be provided by a compact and mobile cryocooler system, developed as a spin-off from the space program. The terahertz HEB imager consists of a computer-controlled optical system mounted on an elevation and azimuth scanning translator which provides a two-dimensional image of the target. We present preliminary measured data at the symposium for a terahertz security system of this type.

Keywords: terahertz frequencies, heterodyne detectors, superconducting devices, hot electron bolometers, focal plane arrays, terahertz imaging

1. INTRODUCTION

Hot electron bolometric (HEB) mixer receivers for terahertz frequencies have been under development during the past ten years. A few instruments based on HEB technology have been deployed or are ready for deployment for astrophysical applications [1,2,3,4]. In astronomical applications, observations of spectral lines have played a major role in expanding our understanding of the interstellar medium and planetary atmospheres. In order to achieve the required sensitivity for astronomical, remote-sensing, homeland security, and biomedical applications, we need to develop receivers operating at sensitivities near the quantum noise limit, and focal plane arrays (FPAs) with multiple mixer elements. HEB mixers, which use nonlinear heating effects in superconductors near their transition temperature, have become an excellent candidate for applications requiring low noise temperatures at frequencies from 0.5 THz to 12 THz. The sensitivity of heterodyne ('mixer') receivers is usually expressed in terms of their double sideband (DSB) receiver noise temperature. The state-of-the-art DSB receiver noise temperatures versus a broad frequency range for different types of terahertz receivers are shown in Figure 1. The quan-

*Work partly supported by the U.S. National Institute of Standards and Technology, not subject to U.S. copyright.

**gerecht@boulder.nist.gov; phone (303) 497-4199; fax (303) 497-3970;

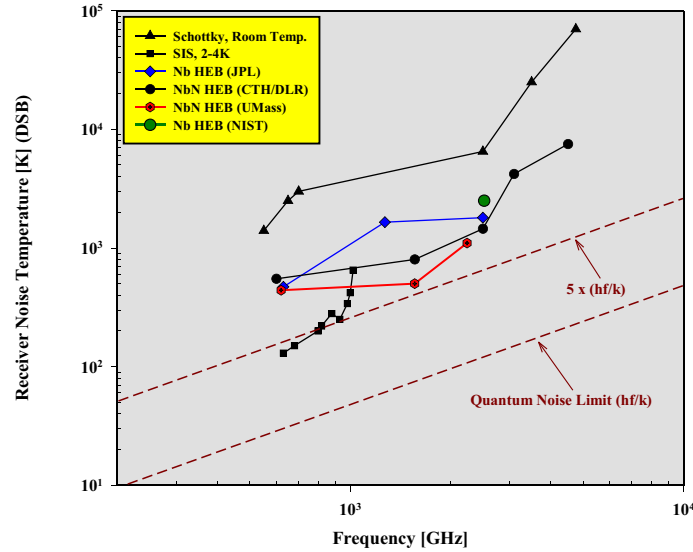


Figure 1: Double sideband receiver noise temperature for different heterodyne receivers over a wide frequency range.

tum noise limit for the DSB system noise temperature (when performing narrow band observations within a single sideband) is hf/k (shown dashed in Figure 1). The DSB receiver noise temperatures of the best receivers from 100 GHz to 2.5 THz approach the $5xhf/k$ line (also shown by dashed line). Superconductor-insulator-superconductor (SIS) mixers have the best sensitivity up to and just above 1 THz, but are limited in frequency by the bandgap frequency of the superconductor material used for the SIS junction. The oldest technology, Schottky-barrier diodes (SBD), yields noise temperatures at terahertz frequencies that are at least an order of magnitude higher than those of hot electron bolometer (HEB) devices and also requires LO power of the order of milliwatts, whereas HEBs require a few hundred nanowatts. This is a very important issue, since high LO power is very difficult to produce at terahertz frequencies.

In addition, imaging and spectroscopy at terahertz frequencies have great potential for both homeland security and healthcare applications. Energy level transitions of important molecules in biology and astrophysics occur at terahertz frequencies. Terahertz radiation (T-rays) can penetrate clothing and, to some extent, can also penetrate biological materials, and because of its shorter wavelengths offers higher spatial resolution than do microwaves or millimeter waves. Both existing direct detector and heterodyne security imaging systems operate at about 100 GHz, and new developments may bring direct detector systems that operate at 350 GHz. Angular resolution is better at higher frequencies with optics of smaller-size. Terahertz HEB imagers are designed with frequencies centered at known atmospheric windows with lower signal degradation. Large FPAs, employing hundreds of HEB elements, promise to provide video rate imaging with superior sensitivities.

2. TERAHERTZ IMAGER WITH HEB DETECTORS

2.1 HEB devices

HEBs are “surface” superconducting devices with extremely small parasitic reactances, even at the highest terahertz frequencies. The device is fabricated from an NbN film, that has been sputtered onto a silicon substrate. The film thickness is typically 3.5 to 4 nm. A typical device size is 4 μm (width) x 0.4 μm (length). An HEB device, integrated with a twin-slot antenna, is shown in Figure 2. The device can be matched to the antenna by changing its aspect ratio. We also use the fact that its impedance at terahertz frequencies (well above the superconducting bandgap frequency) is real and has value equal to its nor-

mal resistance just above the critical temperature. HEB devices are able to absorb the terahertz radiation up to the visible range due to the very short momentum scattering times. HEBs change their resistance as the quasi-particles are heated as a function of the incoming energy. These two properties are independent of the RF/LO frequencies. NbN HEBs have a thermal time constant that is determined by the rate at which phonons are emitted by the electrons, and also by the escape rate of the phonons from the NbN film to the substrate. The resulting conversion gain bandwidth is about 3 to 3.5 GHz for our devices, while the receiver noise temperature bandwidth can be up to twice the gain bandwidth. An operating temperature range for the HEB devices of 4 K to about 6 K is an advantage compared to most other far-infrared (FIR) devices, which require cooling to sub-kelvin temperatures.

2.2 Quasi-optical coupling

The majority of HEB receivers now use quasi-optical coupling to the incoming radiation field by use of a combination of a dielectric lens and an integrated antenna (see Figure 2). We have employed three types of antennas: twin-slot antennas, which have a bandwidth of about 30 %, log-periodic antennas, which can be designed to have several octaves of bandwidth, depending on the number of teeth, and slot-ring antennas (as shown in Figure 3) [5], which allow a more efficient LO injection scheme. The slot-ring antenna has a simpler shape and is easier to fabricate, but does require a filter. The filter works well only if air-bridges (which prevent mode conversion) are inserted as shown in the Figure 3. An additional advantage of this antenna is that the requirement for a diplexer to pump the LO signal into the devices is eliminated. This can be achieved by using different polarizations for the LO beam and the signal beam and coupling both directly to the slot-ring antenna. As far as we know, the fabrication of air bridges has never before been attempted at terahertz frequencies. The slot-ring antenna and the wire grid injection have been demonstrated in our earlier work at 35 GHz, and we have recently fabricated such devices with air bridge filtering on the output CPW [5]. The antennas are produced in an e-beam-evaporated Ti/Au film by lift-off. The signals are in turn coupled to the device through an elliptical lens (4 mm in diameter).

2.3 LO source

We use a CO₂-laser pumped gas laser as an LO source. This system can provide up to 100 mW on the strongest lines, and several tens of milliwatts on a typical line. Although this is much more than the minimum power required, such excess power makes experiments convenient to set up and perform. In order to separate the LO and the signal frequencies, we employ a mylar beam splitter 6 micrometer thick that reflects only about 1 % of the power. We have operated this laser at frequencies close to 5 THz (60 μm). Many lines are available over the frequency range of 1 THz to 5 THz. In the future, harmonic multiplier

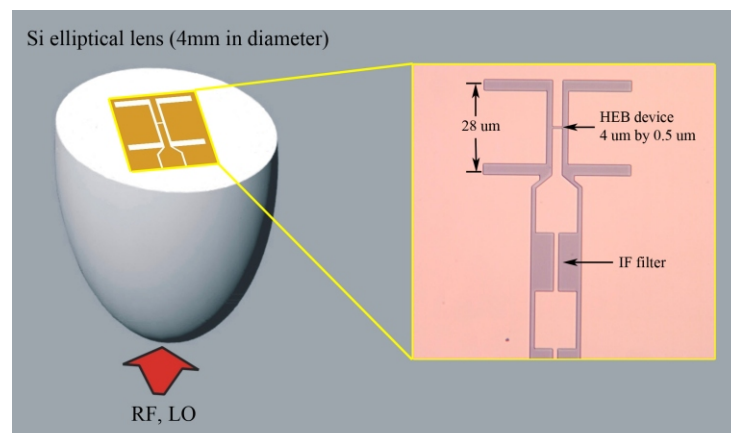


Figure 2: (Left) a quasi-optical design illustration; (right) a photograph of the twin-slot antenna. The HEB device in the center is too small to be seen.

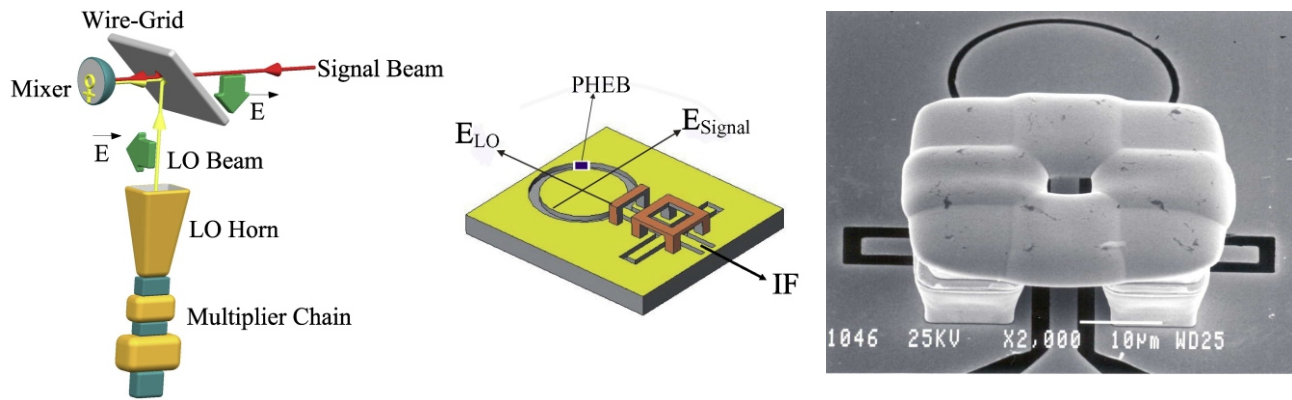


Figure 3: LO injection scheme using a slot-ring antenna and HEB mixer.

sources will replace the laser sources. A number of innovations have produced sources up to 1.9 THz, but with very little power (a few microwatts). At lower frequencies, multiplier sources are becoming available with typical power outputs of hundreds of microwatts.

2.4 IF amplification

To couple the DC signal to the device and extract the IF signal from the device, we use a bias “tee” circuit that is built into the mixer block. We have also developed a broadband MMIC IF amplifier in collaboration with Dr. S. Weinreb of CalTech/JPL [6]. The measured noise temperature of this amplifier is below 8 K over the range of 1-10 GHz. This noise temperature performance is sufficiently low to influence the total HEB receiver noise temperature by not more than a few percent. The amplifier gain is presently about 30 dB. The size of the chip is about 1 mm x 2 mm. We have performed comparative experiments with this amplifier (i) without isolators between it and the HEB device, and (ii) using a series of octave band isolators (the widest ones available). The receiver noise temperature bandwidth (the IF frequency at which the HEB receiver noise temperature has doubled in comparison to the extrapolated value at zero IF) was measured to be 5.5 GHz [7] with the isolators. Remarkably, the amplifier was stable (no oscillation) even when used without isolators. The best noise temperature bandwidth we have achieved with a direct-coupled MMIC IF amplifier is 4.5 GHz. **This shows that it should be feasible to eliminate the isolators in a focal plane array HEB receiver. Note that the isolators are much larger than any other components, and thus cannot be used in multi-element FPAs.**

2.5 Cryogenics

To take full advantage of the HEB technologies, we need cryocoolers capable of extracting >20 mW at 6 K. Relatively low cost, moderate life time, compact cryocoolers exist for >80 K terrestrial applications. Also, long lifetime, compact, maintenance free, relatively high cost, space flight 6 K coolers are under development at Ball Aerospace [8]. Ball Aerospace has developed the basic building blocks for a revolutionary low-temperature (<10 K) cryocooler. The basic cryocooler technology approach uses a hybrid combination of Stirling and J-T thermodynamic cycles. The system uses the mass- and power-efficient Stirling cycle as a precooler to perform the bulk of the cooling to temperatures around 15 K. It then uses the inherently very-low-temperature efficiency of the recuperative (vs. regenerative for the Stirling) J-T cooler to perform the last stages of cooling down to 4 K. Such a system integrated with HEB technology will produce a mobile terahertz imager with superior sensitivities.

2.6 Three-element HEB focal plane array (FPA)

We have developed a 1.6 THz FPA with three HEB elements [9]. The HEB chips are directly integrated with MMIC amplifiers. The concept of the 3 x 1 element array is shown in Figure 4 (top). Three silicon device chips, of the same size (6 x 6 mm), are at the center of the mixer block. On the opposite side of the device chips, 4 mm diameter silicon lenses were attached with purified bees wax. The optical configuration is of the “fly’s eye” type, which allows ample space for the other components in the focal plane. A circuit board accommodates the bias circuitry for the devices as well as for the three MMIC amplifiers (size 1 x 2 mm) in an extension of the single element mixer block concept we have developed [9]. The MMICs are coupled through microstrip lines that include a chip capacitor in series as a DC block. The microstrip lines also function as a matching network to the MMICs. SMA coax lines and connectors allow us to extract the three IF outputs from the sides of this block and three connectors provide all DC bias lines. Figure 4 (bottom) shows photographs of the three-element FPA. Note that no isolator was used in any of our tests. Two of the three elements of the FPA were biased, and LO power was supplied by using a wide laser beam that covered both elements. We found that by defocusing the laser beam until it covered both elements, we could

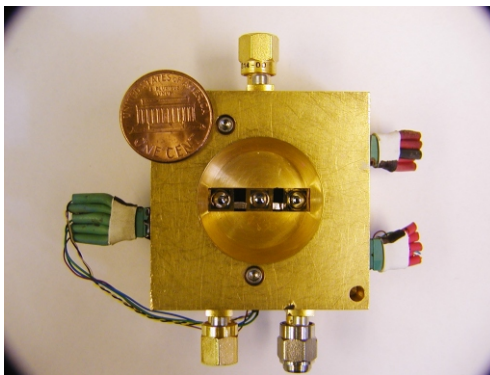
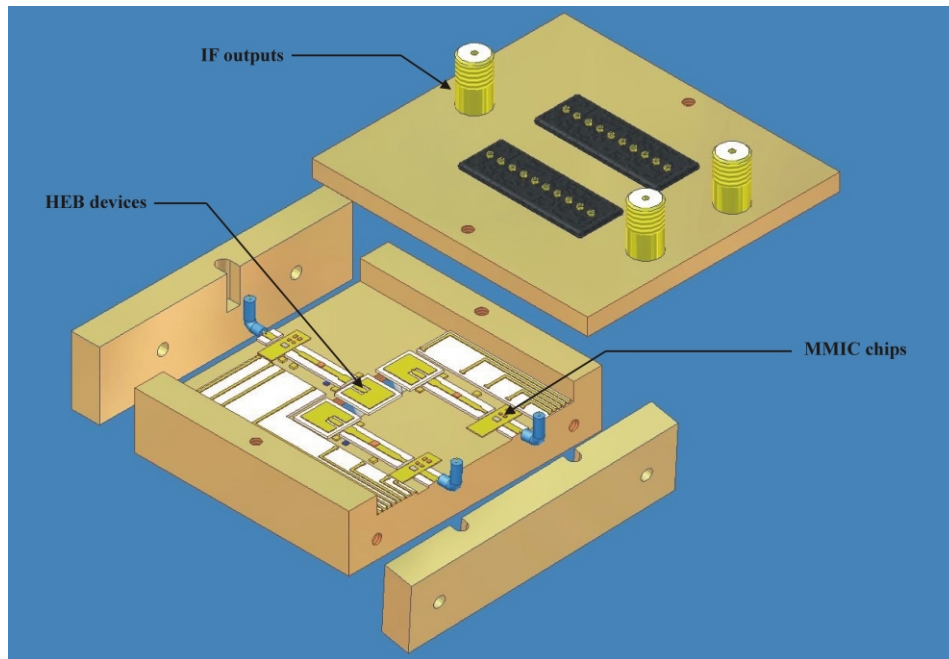


Figure 4: Three-element prototype focal plane array at 1.6 THz. (top) Conceptual design; (bottom) Photographs of the completed FPA unit, which was tested and then delivered to NASA in June, 2004.

easily have enough LO power to pump both elements at the same time. In future systems, more sophisticated LO injection methods will be utilized (see Sec. 4.4). A laser sideband was produced from a second laser. This sideband was focused in the aperture plane of the silicon lenses. The focused sideband beam was then moved with the help of a micrometer driver translator stage, whereupon the output signals from the two elements were recorded on a spectrum analyzer as a function of the position of the sideband beam. We used a convenient IF of 2 GHz in this experiment. The recorded data are shown in Figure 5. The output powers have been normalized to their respective peaks and are plotted on a linear scale. The measured results agree very well with what we would expect. In this prototype array, we used a conservative spacing of the elements. Other work, however, has demonstrated that the “fly’s eye” array configuration can be used at full beam efficiency down to a spacing that corresponds to one 3 dB beamwidth, equivalent to diffraction-limited imaging. The performance of the FPA, first of its kind for frequencies above 1 THz, demonstrates the suitability of HEBs as mixer elements in a much larger FPA imager in the future.

3. HETERODYNE AND DIRECT DETECTORS COMPARISON

The choice between an imager based on heterodyne detectors or direct detectors is not an easy one. Depending on the application, a designer can tailor the instrument to perform better by understanding the similarities and differences of the two types of detectors. Some applications dictate the type of detector to be used. In order to promote understanding of the figures of merit of both detector technologies, a summary of a direct comparison is given in TABLE I. In general, in order to resolve magnitude and phase of a signal, a heterodyne detector should be chosen. A heterodyne detection system down-converts the signal into an intermediate frequency (IF) and requires a local oscillator source. For a higher spectral resolution, heterodyne detector technology is preferable. The figure of merit for sensitivity of direct detectors is the noise equivalent power (NEP) whereas noise temperature is used for heterodyne detectors. The distinction between system noise temperature and receiver noise temperature is that the former includes the noise from the input source (ideally the vacuum fluctuations), whereas the latter includes the noise generated in the receiver only. Obviously, it is the system noise temperature that determines the sen-

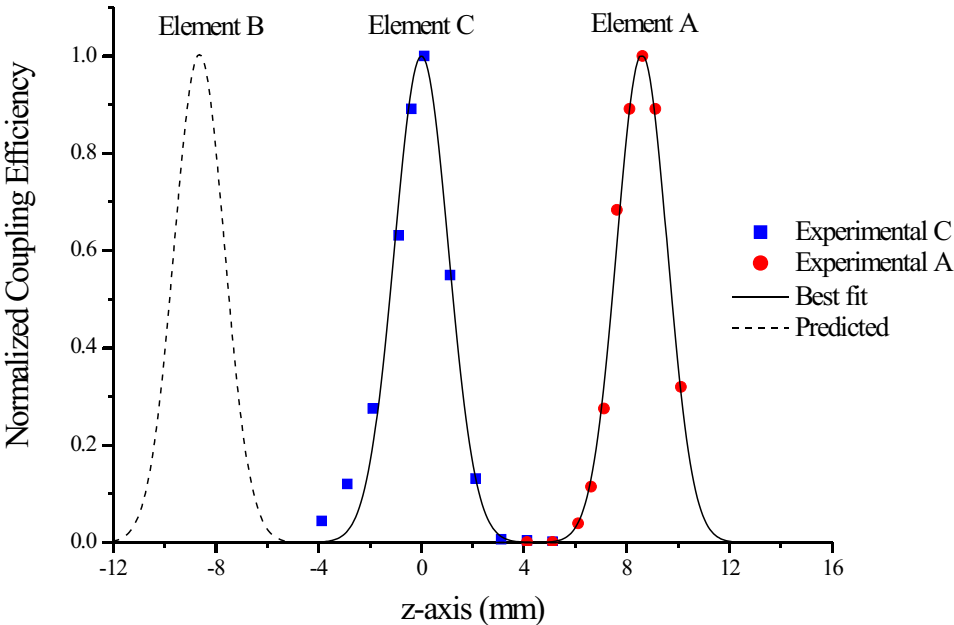


Figure 5: Measured response of two adjacent elements in the FPA.

TABLE I
SUMMARY OF NOISE FIGURES OF MERIT

Heterodyne Detector	Direct Detector
<p><i>HEB (Hot Electron Bolometer) Mixer:</i></p> <p><i>DSB Noise temp. ~ 900 K (at 4-6 K)</i></p> <p><i>Bandwidth 4 GHz</i></p> <p>$T_{RMS} = T_{sys}/\sqrt{B} = 0.045 \text{ K in } 0.1 \text{ sec}$</p> <p><i>or 0.014 K (14 mK) in 1 sec</i></p> <p><i>SBD (Schottky Barrier Diode) Mixer:</i></p> <p><i>DSB Noise temp. ~ 3,600 K (at room temp.)</i></p> <p><i>Bandwidth 12 GHz</i></p> <p>$T_{RMS} = T_{sys}/\sqrt{B} = 0.1 \text{ K in } 0.1 \text{ sec}$</p> <p><i>HEB and SBD are quite similar in terms of sensitivity.</i></p> <p>$NEP_{HEB} (1 \text{ sec}) = k B T_{RMS} = 7.8 \cdot 10^{16} \text{ W}/\sqrt{\text{Hz}}$</p> <p>$NE T_{HEB} = 1 \text{ sec} \quad T_{RMS} = 14 \text{ mK}$</p>	<p><i>Nb room temperature detector [10]:</i></p> <p><i>Frequency about 100 GHz</i></p> <p><i>Active system (IMPATT at 1W peak)</i></p> <p>$NEP_{Nb} (1 \text{ sec}) = 5 \cdot 10^{11} \text{ W}/\sqrt{\text{Hz}}$ at room temp.</p> <p><i>Improved $NEP_{Nb} (1 \text{ sec}) = 5 \cdot 10^{12} \text{ W}/\sqrt{\text{Hz}}$ at room temp.</i></p> <p>$NEP_{Nb} (1 \text{ sec}) = 1.4 \cdot 10^{14} \text{ W}/\sqrt{\text{Hz}}$ at 4 K [11]</p> <p><i>NE T_{Nb} = NEP_{Nb}/(k B) in 1 sec integration time</i></p> <p><i>Assume bandwidth 70 GHz (optimistic)</i></p> <p><i>For $NEP_{Nb} = 5 \cdot 10^{11} \text{ W}/\sqrt{\text{Hz}}$, NE T_{Nb} = 52 K</i></p> <p><i>For $NEP_{Nb} = 5 \cdot 10^{12} \text{ W}/\sqrt{\text{Hz}}$, NE T_{Nb} = 5.2 K</i></p> <p><i>For $NEP_{Nb} = 1.4 \cdot 10^{14} \text{ W}/\sqrt{\text{Hz}}$, NE T_{Nb} = 14 mK</i></p>

sitivity of a heterodyne detector system in an imaging application. In order to compare the sensitivity of a heterodyne detector with a direct detector used in an active imaging system (the target is illuminated), the noise temperature of the heterodyne detector has to be converted to noise equivalent power (see TABLE I). Detectors for passive systems are characterized by their noise equivalent difference in temperature (NE T). TABLE I compares these figures of merit (NEP, NE T) for existing detector technologies. In general, cooling a detector improves its sensitivity (lowers its intrinsic noise). Direct detectors made of Nb show, when cooled to 4 K, an improvement of about three orders of magnitude in their NEP performance [11]. Such NEP values (see TABLE I) are reported for frequencies below 350 GHz. Such detectors cannot be used at higher frequencies, whereas HEB detectors can be used over the entire terahertz range with similar performance. As shown above, the NEP performance for an HEB detector is better by two orders of magnitude than that of an Nb direct detector at the same operating temperature (liquid helium temperature). The NE T values for both types of detectors are virtually the same for a signal integration time of 1 second and a bandwidth of operation for the Nb direct detector of 70 GHz. Such bandwidth is optimistic and is a function of the antenna element used for coupling the signal. At 350 GHz, the bandwidth assumed for this calculation is 20 % and is difficult to achieve. For shorter integration time (say 0.1 sec), the NE T for the HEB increases by a factor of $\sqrt{10}$, whereas NE T for the Nb direct detector will increase by a larger factor, since the noise in the latter is dominated by a 1/f process. This is important since imaging systems of the type we consider for security applications must be operated at quite short integration times in order to obtain imaging frame rates similar to video rates. One clear advantage of the direct detectors used in imaging is the lack of LO source requirement.

4. IMAGING WITH HEB FOCAL PLANE ARRAYS

4.1. Introduction

The technology for designing and constructing focal plane arrays with heterodyne HEB elements was described above. Prototypes using this technology have been studied sufficiently that we can now design and develop imaging systems utilizing such arrays. Existing imaging systems [12,13] for security applications are limited to frequencies near 100 GHz, and are best suited to imaging at relatively close range (say ~ 3 m). It is highly desirable, however, to also be able to extend the capability of detecting concealed weapons through imaging with high resolution (about 1 cm) at greater distances (~ 25 m). As noted above, systems operating at 100 GHz would require optics of impractically large size in order to achieve the required resolution at the larger distances, so that we naturally want to consider terahertz systems that employ wavelengths about an order of magnitude shorter. While the resolution increases as we continue to increase the frequency, there are other considerations that result in a frequency close to 850 GHz being optimum. This choice is based on the increasing attenuation of terahertz waves due to water vapor in the atmosphere and also on the relatively high attenuation of typical clothing materials above 1 THz [14]. Typical desired characteristics of a terahertz security imaging system may be summarized as follows:

- (1) **Spatial resolution of 1cm across a 2 m by 1 m target at a distance of 25 m; the total number of pixels then is 2×10^4 .**
- (2) **Temperature resolution of 1K (RMS).**
- (3) **Acquisition time of a full image compatible with video rates, in the range 30 ms to 100 ms.**

Since an array with 2×10^4 elements is not presently feasible, we must consider a combination of scanning and an FPA with the required number of elements to meet the above requirements. We will now consider how these requirements can be fulfilled.

4.2. Estimate of imaging system parameters

System noise temperature and bandwidth:

NbN HEB mixers have demonstrated a double sideband (DSB) receiver noise temperature of 400-500 K at 850 GHz [15]. In a terrestrial application, the temperature of the environment will add 300 K to the receiver noise temperature when calculating the system noise temperature. Furthermore, there will be atmospheric attenuation and attenuation of the system components between the object and the receiver. We therefore estimate an effective system noise temperature (T_{SYS}) of 900 K over the entire IF band and an effective system bandwidth (B) of 3.9 GHz .

Integration time and array size:

The RMS fluctuations in the measured radiation temperature (see Section 3) are given by

$$T_{RMS} = \frac{T_{SYS}}{\sqrt{B_{eff}}} = \frac{900}{\sqrt{3.9 \times 10^9}} \text{ K}. \quad (1)$$

Here, t is the integration time in which the receiver elements produce an RMS fluctuation of 1 K, and B_{eff} is the effective bandwidth (defined such that it can be used in Eq. (1), taking into account the measured HEB noise temperature versus IF). Eq. (1) assumes that any fluctuations at the receiver output, due to gain fluctuations, have been cancelled by employing a suitable switching scheme (see below in Sec. 4.3). From Eq. (1) we find $t = 2.08 \times 10^{-4}$ sec. For a frame time of 30 ms, we can produce $3 \times 10^{-2} / 2.08 \times 10^{-4} = 144$ images by raster scanning. In order to produce a total of 2×10^4 pixels, the array needs to

have $2 \times 10^4 / 144 \sim 140$ elements. A square FPA of 196 (14 x 14) elements will produce the required $T_{\text{RMS}} = 1 \text{ K}$ with some margin for down time during scanning operations. The cross-sectional size of the array will be very compact, about 7.7 cm by 7.7 cm, assuming that each element occupies 5.5 mm x 5.5 mm. Smaller arrays are feasible if (i) the total target area, (ii) the frame time, and/or (iii) the spatial resolution requirements may be relaxed. For example, the 650 GHz system used in reference [16] identified a gun-like object under clothing in an image of 6,500 pixels. At 25 m distance and 2 m x 1 m target size this would correspond to a resolution of 1.75 cm. If we also relax the frame time to 100 ms, we estimate that 480 images must be produced by scanning. The 6,500 pixel image could be obtained by use of a linear scan of a $6,500/480 = 14$ element linear array. The linear array would need to perform limited raster scanning as well, to cover the entire width of the target (the width of the target would be about 57 pixels). The linear geometry of this FPA would simplify the array architecture considerably. This linear array would be about 7.7 cm long. Clearly, a range of other array sizes and geometries are possible, depending on the actual specifications of the imaging system. The linear array would also simplify the scanning process. In the case of a square array, the raster scanning technique would require switching the outputs between individual rows of elements after the array has scanned past one row of pixels.

4.3. Optical considerations

In order to achieve optimum spatial resolution, we need to focus the system at the desired distance. A calculation using Gaussian optics shows that at 850 GHz the main optical element needs to have a diameter of about 25 cm to produce a focused spot of 1 cm diameter, while a 1.75 cm spot needs optics of only about 15 cm diameter. A Cassegrain type of optical system is compact and has excellent off-axis properties.

The optical system will also have to include some means of canceling system gain fluctuations, such as chopping between the target and a load held at a constant temperature. We have studied the spectrum of the gain fluctuations in our HEB detectors, using the Allan variance technique [17]. The fluctuations at high frequencies (typically higher than 1 Hz) are Gaussian, and correspond to white noise. Slower gain fluctuations typically have a $1/f$ character, and if the Allan variance is plotted as a function of the correlation time (T), we then find that it varies as $1/T$ for short times, and has a “break-point” at which it stops decreasing, becomes “flat”, and then sometimes increases at even larger values for T [17]. If the device is operated in the $1/T$ region, the noise will “integrate down” as the integration time increases. The “break point” between $1/T$ behavior and flat T-dependence, is called “the Allan time (T_A)”. We measured the Allan variance for one of our detectors for an IF bandwidth of 80 MHz [18], and obtained an Allan time of about 1 second, which is typical for NbN devices of the same size ($0.4 \text{ m} \times 4 \text{ m}$). The effective integration time of a particular pixel in an imaging system will be much shorter, however, since (i) the bandwidth is much wider (about 3 GHz) and (ii) each pixel has to produce its signal in a period determined by considerations described in Sec. 4.4. Optimizing the Allan variance and understanding the physical causes of the different processes contributing to it, then become of paramount importance.

4.4. LO power injection

Recent careful measurements of the LO power required for similar NbN HEB devices indicate a power level of about 1.6 W for a device size of $0.4 \text{ m} \times 4 \text{ m}$ (power estimated outside the mixer block, but inside the dewar) [19]. Smaller devices need less power, but have somewhat inferior properties in terms of noise temperature, stability, and life-time. The optical losses through the dewar window and thermal filters are at most 3 dB. The total power required for a 196-element array then is about 600 W, and for the 14-element linear array about 40 to 50 W. Commercial harmonic multiplier sources are presently available with output powers of 100 W, and these can be expected to increase in power in the near future. Lasers and backward-wave oscillators have output powers of many milliwatts, but are much more bulky, so the long-term solution is clearly to use a multiplier source. A trade-off may also have to be made between device size, noise temperature and LO power. The

LO power will be injected with very low losses by coupling the LO and signal beams quasi-optically in orthogonal polarizations through the silicon lenses to slot-ring antenna elements (see Sec. 2.2). A simple wire grid can be used as the diplexer. Other alternatives are to use a silicon etalon for LO injection. Directing the LO power equally to a number of elements is a problem that has been solved elegantly through the use of a Fourier grating reflector [20].

4.5. Experiments with a Single Element Scanned System

The prototype FPA we have demonstrated at 1.6 THz indicates that the problems of constructing larger versions of such arrays can be solved. We also need to verify that such a system will actually produce useful images. This part of the project can be accomplished by scanning the radiation from a target to a single-element HEB mixer detector. We have constructed such a system at 1.6 THz. The imaging system uses a standard electromagnetic actuator to rotate a plane mirror by about 15 degrees at a rate of 7 Hz. A target area located about 5 cm from the scanning mirror is selected by the scanning mirror, and focused through two offset-axis paraboloid (OAP) mirrors onto the HEB detector inside a liquid helium dewar. The total IF power is filtered to contain the IF band from 1 GHz to 4 GHz and detected in a standard microwave detector. The detected signal can either be observed on a lock-in amplifier (which in this case effectively yields a single point image), or displayed and averaged on a digital oscilloscope. In the latter case, we obtain a linear image of one line in the target. Using this technique, we have recorded the image of a step (located in about the middle of the scanned length) from a room temperature load to a liquid nitrogen temperature load, shown in Figure 6. Such recordings enable us to calibrate the temperature scale in the image. At this preliminary stage, the system is sensitive to mechanical vibrations transmitted to the optical table from the scanning mirror mechanism. These give rise to the main part of the noise visible in the recording. We also detect the signal on the lock-in amplifier, which yields a stable output and is not sensitive to mechanical vibrations. Any noise outside the frequencies we are interested in will be filtered out in an eventual system. Even at this preliminary stage, the system can detect temperature differences much smaller than what is shown in Figure 6. For example, we have recorded linear images of metal bars (also covered by a shirt) seen against a background of room temperature absorber material, as well as human hands against the same background. The spatial resolution agrees with what can be expected based on optical considerations.

5. CONCLUSIONS AND FUTURE WORK

We have achieved the first demonstration of a low-noise heterodyne focal plane array operating at a frequency above 1 THz (1.6 THz). The prototype array has three elements consisting of NbN HEB detectors on silicon substrates. We use a quasi-op-

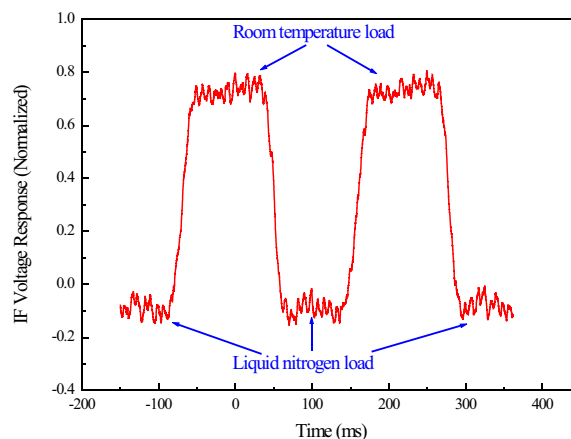


Figure 6: Image of a step from a room temperature load to a liquid nitrogen temperature load.

tical design to couple the signal and LO power to the detectors. We also produced a figures-of-merit comparison in order to demonstrate the clear advantage of heterodyne detectors in terahertz imaging systems. A single-pixel HEB array was used to image different targets. Preliminary imaging results of terrestrial objects are very promising. An analysis of a larger element array shows that video-rate imaging, using the HEB technology, is feasible.

Figure 7 illustrates a conceptual design for an FPA with multiple HEB devices. This design can be extended to a large number of elements. Initially, the architecture shown here will be implemented for a small number of elements. The lenses and HEB elements will be configured in the same fly's eye arrangement that we used in the prototype FPA. Since the lenses can be stacked much closer than in the prototype with only a small clearance, the angular resolution of the array produced on the sky will be only slightly larger than one diffraction-limited beamwidth (FWHM). This is close to the optimal obtainable with any FPA. The MMIC IF amplifiers will be assembled on a separate substrate and contacted through via holes. As an alternative, this substrate will be attached to a cooling stage at 15-20 K, in order to improve the cooling requirements of the array. The amplifiers would then be contacted through coplanar waveguide or microstrip lines on flexible Kapton ribbons. This general architecture is well suited for integration of a mobile terahertz imager with superior sensitivities.

ACKNOWLEDGMENTS

This work was supported by NASA through grant NRA-00-01-SARA-012 to NIST and UMass/Amherst, and contract NAS1-01058 to UMass/Amherst.

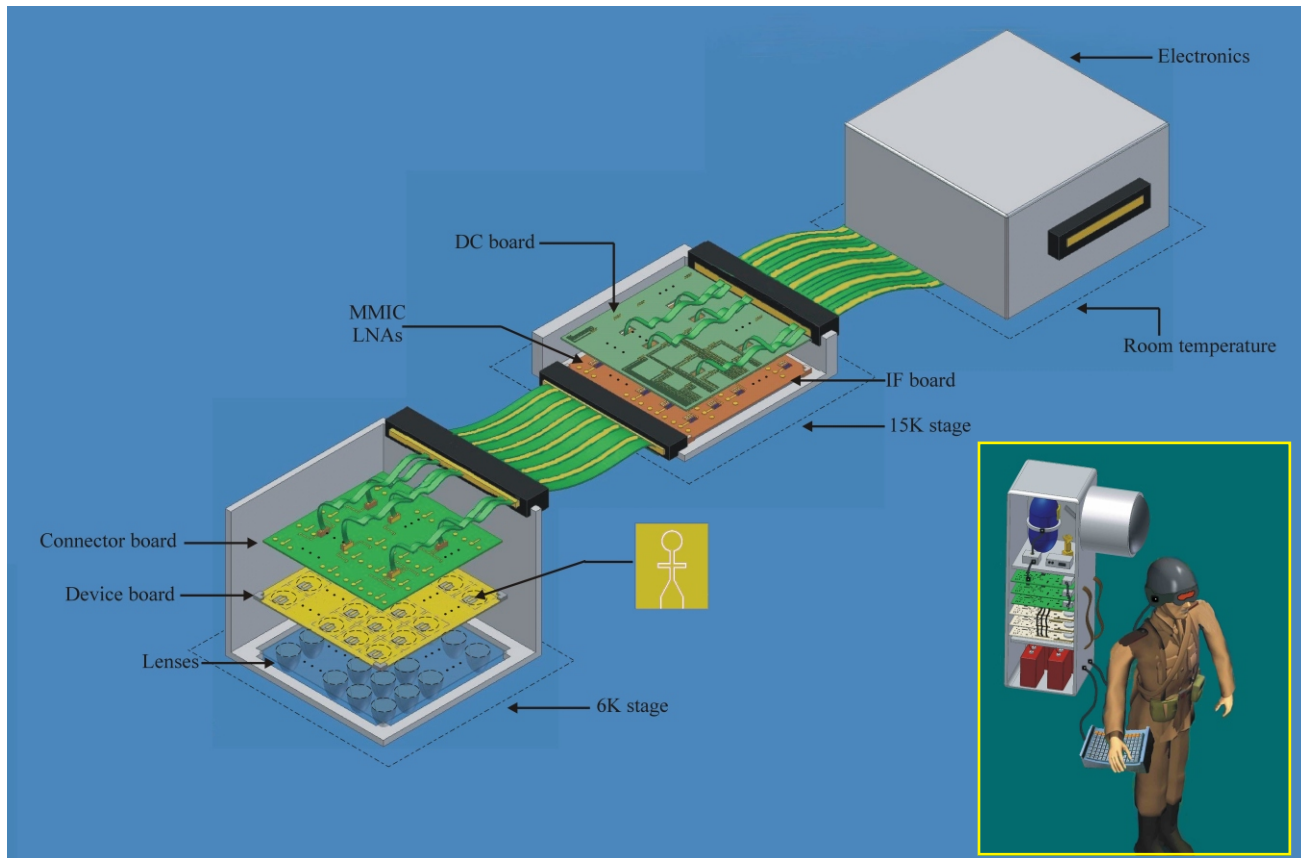


Figure 7: A conceptual configuration for a terahertz heterodyne focal plane array with HEB devices.

REFERENCES

1. E. Gerecht, S. Yngvesson, J. Nicholson, Y. Zhuang, F. Rodriguez Morales, X. Zhao, D. Gu, R. Zannoni, M. Coulombe, J. Dickinson, T. Goyette, W. Gorveatt, J. Waldman, P. Khosropanah, C. Groppi, A. Hedden, D. Golish, C. Walker, J. Kooi, R. Chamberlin, A. Stark, C. Martin, R. Stupak, N. Tothill and A. Lane, "Deployment of TREND – A Low Noise Receiver User Instrument at 1.25 THz to 1.5 THz for AST/RO at the South Pole". 14th Intern. Symp. Space THz Technology, Tucson, Az, Apr. 2003.
2. J. Kawamura et al., "First Light with an 800 GHz Phonon-Cooled HEB Mixer Receiver," p. 35-43, 9th ISSST, (1998).
3. S. Radford, "CO(9-8) in Orion," 14th Intern. Symp. Space THz Technology, Tuscon, AZ, (April 2003).
4. S. Cherednichenko, M. Kroug, N. Wadefalk, P. Khosropanah, A. Adam, H. Merkel, E. Kollberg, D. Loudkov, B. Voronov, G. Gol'tsman, H.-W. Huebers, H. Richter, "1.6 THz HEB mixer for far infrared space telescope (Herschel)", to be published in Physica C (2003).
5. E. Gerecht, D. Gu, X. Zhao, J. Nicholson, F. Rodriguez- Morales, S. Yngvesson, "Development of NbN Terahertz HEB Mixers Coupled Through Slot Ring Antennas", 15th Intern. Symp. Space THz Technol., Northampton, MA, April 27-29, 2004.
6. D.R. DeBoer and D.-J. Bock, "The Allen Telescope Array: Splitting the Aperture," IEEE Microwave Magazine, 5, 46 (2004).
7. F. Rodriguez-Morales and S. Yngvesson, "Impedance and Bandwidth Characterization of NbN Hot Electron Bolometric Mixers," 14th Intern. Space Terahertz Technol. Symp., Tuscon, AZ (2003).
8. Glaister, D. S., Gully, W. J., Marquardt, E., Stack, R., "Low Temperature Space Cryocoolers at Ball Aerospace", Space Cryonics Workshop, Alyeska, AK, July, 2003.
9. F. Rodriguez-Morales, K.S. Yngvesson, E. Gerecht, N. Wadefalk, J. Nicholson, D. Gau, X. Zhao, T. Goyette, and J. Waldman, "A Terahertz Focal Plane Array Using HEB Superconducting Mixers and MMIC IF Amplifiers," to appear in IEEE Microwave and Wireless Components Letters (2005).
10. S. Nolen, J.A. Koch, N.G. Paulter, C.D. Reintsema, and E.N. Grossman, "Antenna-Coupled Bolometers for Millimeter-Wave Imaging Arrays," Proc. SPIE 3795 (1999).
11. A. Luukanen and J.P. Pekola, "A Superconducting Antenna-Coupled Hot-Spot Microbolometer, Appl. Phys. Lett., 82, 3970 (2003).
12. P.F. Goldsmith, C.-T. Hsieh, G.R. Huguenin, J. Kapitzky, and E.L. Moore, "Focal Plane Imaging Systems for Millimeter Wavelengths," "IEEE Trans. Microw. Theory Techniques, MTT-41, 1993.
13. E.N. Grossman, S. Nolen, N.G. Paulter, and C.D. Reintsema, "Concealed Weapon System Using Uncooled, Pulsed, Imaging Arrays of Millimeter Wave Bolometers," Proc. SPIE Vol. 4373, 7 (2001).
14. J.E. Bjarnarson, T.L.J. Chan, A.W.M. Lee, M.A. Celis, and E.R Brown, "Millimeter Wave, Terahertz, and Mid-Infra-red Transmission Through Common Clothing," Appl. Phys. Lett., 85, 519 (2004).
15. S. Yngvesson, "Review of HEB Heterodyne Detectors and Receiver Systems for the THz Range: Present and Future", 14th Intern. Symp. Space THz Technology, Tucson, Az, (2003).
16. R.J. Dengler, A. Skalare, and P.H. Siegel, "Passive and Active Imaging of Humans for Contraband Detection at 640 GHz," 2004 IEEE MTT-S Digest, 1591.
17. J. Kooi, G. Chattopadhyay, M. Thielman, T. Phillips, and R. Schieder, "Noise Stability of SIS Receivers," Int J. IR and MM Waves, vol. 21, 2000.
18. Fernando Rodriguez-Morales and S. Yngvesson, "Integrated THz Receivers Based on NbN HEB Mixers and InP MMIC IF Amplifiers", Paper submitted to the 2005 IEEE Intern. Microwave Symp.
19. J. Kooi, S. Cherednichenko et al, private communication, 2004.
20. S. Heyminck and U.U. Graf, "A ray-Receiver LO Unit Using Collimating Fourier Gratings", SPIE Proc. 12th Intern. Symp. Space THz Technol., San Diego, 263 (2001).